IEEE Access
Multidisciplinary ⋮ Rapid Review ⋮ Open Access Journal

Received February 12, 2020, accepted March 4, 2020, date of publication March 16, 2020, date of current version March 26, 2020.

Digital Object Identifier 10.1109/ACCESS.2020.2981249

Rapid Optimization of Compact Microwave Passives Using Kriging Surrogates and Iterative Correction

SLAWOMIR KOZIEL[1,2], (Senior Member, IEEE), AND ANNA PIETRENKO-DABROWSKA[2], (Member, IEEE)

[1]Engineering Optimization and Modeling Center, Department of Engineering, Reykjavik University, 101 Reykjavik, Iceland
[2]Faculty of Electronics, Telecommunications and Informatics, Gdańsk University of Technology, 80-233 Gdańsk, Poland

Corresponding author: Slawomir Koziel (koziel@ru.is)

This work was supported in part by the Icelandic Centre for Research (RANNIS) under Grant 174114051, and in part by the National Science Centre of Poland under Grant 2015/17/B/ST6/01857.

ABSTRACT Design of contemporary microwave components is—in a large part—based on full-wave electromagnetic (EM) simulation tools. The primary reasons for this include reliability and versatility of EM analysis. In fact, for many microwave structures, notably compact components, EM-driven parameter tuning is virtually imperative because traditional models (analytical or network equivalents) are unable to account for the cross-coupling effects, strongly present in miniaturized layouts. At the same time, the cost of simulation-based design procedures may be significant due to a typically large number of evaluations of the circuit at hand involved. In this paper, a novel approach to expedited design closure of compact microwave passives is presented. The proposed procedure incorporates available designs (e.g., existing from the previous design work on the same structure) in the form of the kriging interpolation models, utilized to yield a reasonable initial design and to accelerate its further refinement. An important component of the framework is an iterative correction procedure that feeds the accumulated discrepancies between the target and the actual design objective values back to the kriging surrogate to produce improved predictions. The efficacy of our methodology is demonstrated using two miniaturized impedance matching transformers with the optimized designs obtained at the cost of a few EM simulations of the respective circuits. The relevance of the iterative correction is corroborated through the comparative studies showing its superiority over rudimentary gradient-based refinement.

INDEX TERMS Microwave design, design closure, parameter tuning, kriging interpolation, iterative correction, EM-driven design, compact circuits.

I. INTRODUCTION

The involvement of computational models in the design of microwave components, primarily full-wave electromagnetic (EM) simulation tools, has been steadily growing over the recent years. Some of the clear advantages of EM analysis include versatility and evaluation reliability. At the same time, full-wave simulations might be associated with considerable computational overhead, which is normally acceptable for design verification but may become prohibitive whenever multiple analyses are required. The primary design task entailing a large number of simulations is (local) parametric optimization [1], others, even more demanding include global search procedures [2], uncertainty quantification [3], or yield-driven design [4].

The aforementioned challenges of EM-driven design are particularly pertinent to miniaturized microwave components (couplers, power dividers, filters, impedance matching transformers [5]–[7]), where conventional transmission lines (TLs) are folded [8] or replaced by physically smaller building blocks (e.g., compact cells employing the slow-wave phenomenon [9], [10]). Furthermore, compact structures often incorporate defected ground structures (DSGs) [11] or multi-layer implementations [12]. One of the issues associated with such structures are considerable cross-coupling effects, only accountable for through the EM analysis.

The associate editor coordinating the review of this manuscript and approving it for publication was Lei Jiao.

This makes EM-driven parameter tuning a mandatory stage of the design process. Additional difficulties arise due to a typically large number of geometry parameters that need to be handled. These do not only result from the said compact realizations but also additional functionalities the circuits are to be designed for (e.g., multi-band operation [13], harmonic suppression [14]).

Addressing the aforementioned issues, in particular, accelerating EM-driven design procedures has been extensively addressed in the literature. A conceptually straightforward approach (yet complex implementation-wise) is to incorporate adjoint sensitivities into gradient-based algorithms [15], [16] although availability of this technology is limited throughout commercial simulation packages. Another strictly algorithmic method is to suppress finite-differentiation sensitivity updates, e.g., by monitoring Jacobian variability [17] or design relocation [18]. In recent years, utilization of fast surrogate models has been gaining considerable popularity. In the context of global optimization, data-driven surrogates combined with sequential sampling schemes are often used (e.g., efficient global optimization (EGO)-type of methods [19]). On the other hand, in the context of local optimization, physics-based surrogate-assisted frameworks have been employed as well. Example methods include space mapping [20], adaptive response scaling [21], or feature-based optimization [22], some of which involve variable-fidelity EM simulation models.

In many practical cases, a number of previously obtained designs of a given microwave structure are available, e.g., optimized for various operating frequencies or substrate parameters. Utilization of such designs is another option for speeding up the optimization process. The problem-specific knowledge can be encoded into the design curves [23], determining the relationships between the system (e.g., geometry) parameters and figures of interest (operating frequencies, bandwidth, power split ratio). This allows for a rapid identification of at least a reasonable starting point for further refinement. The recently proposed techniques involving inverse surrogate models [24] offer a more comprehensive treatment, i.e., rendering good initial designs (with respect to selected performance figures) and design refinement within the same framework. Some variations of these methods work in variable-fidelity simulation setups [9] as well as permit low-cost parameter tuning with respect to performance figures not directly handled by the inverse surrogates [25].

The purpose of this paper is an introduction of a simple yet reliable technique for expedited design optimization of compact microwave components. The proposed approach employs kriging interpolation surrogates constructed from a set of pre-existing designs. The models are utilized to yield a good initial design as well as to estimate the sensitivities of the component outputs therein. An iterative correction procedure is subsequently applied to refine the design by feeding the accumulated deviations between the actual and the target performance figure values back to the surrogate model. Our methodology is comprehensively validated using two miniaturized impedance matching transformers optimized for various design scenarios over wide ranges of operating frequencies. In all considered cases, optimized solution is obtained at the cost of a few EM analyses of the respective transformer structure. At the same time, the advantages of the iterative correction over a rudimentary design refinement via local gradient search are demonstrated.

II. EXPEDITED MICROWAVE DESIGN CLOSURE USING KRIGING SURROGATES AND ITERATIVE CORRECTION

In this section, the proposed surrogate-assisted optimization procedure is formulated. Its basic ingredients are kriging interpolation metamodels constructed using available designs, as well as the iterative correction scheme. The surrogates permit generation of a reasonable starting point and estimation of the component response sensitivities therein, whereas the correction procedure enables low-cost design refinement.

A. PARAMETER AND OBJECTIVE SPACE. DESIGN CLOSURE TASK FORMULATION

The vector of designable geometry parameters of the microwave component of interest will be denoted as $\boldsymbol{x} = [x_1 \ldots x_n]^T$. The parameter space X is typically determined by the lower and upper bounds for $\boldsymbol{x}$. The performance figures (including the operating conditions), the circuit is to be designed for, will be denoted as F_k, $k = 1, \ldots, N$. The examples include center frequency, bandwidth, power split ratio, but also parameters (permittivity, height) of the substrate the structure is to be implemented on. The objective space F is then defined as containing the vectors $\boldsymbol{F} = [F_1 \ldots F_N]^T$ and delimited using their ranges $F_{k.\min} \leq F_k \leq F_{k.\max}$. The interval $F = [F_{1.\min}\ F_{1.\max}] \times \ldots \times [F_{N.\min}\ F_{N.\max}]$ determines the intended region of validity of the optimization procedure.

Let $\boldsymbol{R}(\boldsymbol{x})$ stand for the output of the computational (here, EM-simulation) model of the circuit at hand, e.g., S-parameters versus frequency, at the design $\boldsymbol{x}$. The design closure task is to improve the circuit performance by solving the minimization problem

$$\boldsymbol{x}^* = \arg\min_{\boldsymbol{x}} U(\boldsymbol{R}(\boldsymbol{x}), \boldsymbol{F}) \tag{1}$$

where U is the scalar merit function.

For the sake of illustration, let us consider a dual-band impedance transformer with its reflection to be minimized over the frequency bands $f_{k.1}$ to $f_{k.2}$, $k = 1, 2$. In this case, the vector of operating conditions could be $\boldsymbol{F} = [F_1\ F_2\ F_3\ F_4]^T = [f_{1.1}\ f_{1.2}\ f_{2.1}\ f_{2.2}]^T$, and the merit function may be defined as

$$\begin{aligned} &U(\boldsymbol{R}(\boldsymbol{x}), \boldsymbol{F}) \\ &= U(S_{11}(\boldsymbol{x}), \boldsymbol{F}) \\ &= \max\left\{\max_{f_{1.1} \leq f \leq f_{1.2}} \{|S_{11}(\boldsymbol{x}, f)|\}, \max_{f_{2.1} \leq f \leq f_{2.2}} \{|S_{11}(\boldsymbol{x}, f)|\}\right\} \end{aligned} \tag{2}$$

B. PRE-EXISTING DESIGNS AND KRIGING SURROGATES

The prerequisite for the proposed design closure framework is the existence of designs $\boldsymbol{x}_b^{(j)}$, $j = 1, \ldots, p$, pre-optimized (according to (1)) with respect to the selected objective vectors $\boldsymbol{F}^{(j)} = [F_1^{(j)} \ldots F_N^{(j)}]^T$. These vectors may be known beforehand, e.g., from the previous design work on a given component or obtained specifically to initialize the design procedure.

Furthermore, we denote by $\boldsymbol{J}_b^{(j)} = \boldsymbol{J}(\boldsymbol{x}_b^{(j)})$, $j = 1, \ldots, p$, the Jacobians of $\boldsymbol{R}(\boldsymbol{x}_b^{(j)})$. These are normally obtained as a by-product of solving (1) when $\boldsymbol{x}_b^{(j)}$ were found using gradient search; otherwise, sensitivity can be estimated through finite differentiation.

The reference designs are used to construct two kriging interpolation [26] surrogates:

- $s_x(\boldsymbol{F})$ – the model defined over the objective space F with the outputs in the parameter space X; the training data set for $s_x(\cdot)$ is $\{\boldsymbol{F}^{(j)}, \boldsymbol{x}_b^{(j)}\}_{j=1,\ldots,p}$;
- $s_J(\boldsymbol{F})$ – the model defined over the objective space F with the values in the space of the component response sensitivities; here, the training data is $\{\boldsymbol{F}^{(j)}, \boldsymbol{J}_b^{(j)}\}_{j=1,\ldots,p}$.

A conceptual illustration of the objective space, the meaning of the reference designs, as well as the kriging surrogates have been shown in Fig. 1 for an exemplary miniaturized impedance matching transformer.

C. INITIAL DESIGN

The set $s_x(F)$ of all points of the form $s_x(\boldsymbol{F})$, $\boldsymbol{F} \in F$ (also referred to as the image of the objective space through s_x) approximates the set $O(F)$ consisting of the designs that are optimum in the sense of (1) for all $\boldsymbol{F} \in F$. Consequently, the point

$$\boldsymbol{x}^{(0)} = s_x(\boldsymbol{F}_t) \tag{3}$$

is the best initial design corresponding to a target vector $\boldsymbol{F}_t$ that can be obtained from the information contained in the designs $\boldsymbol{x}_b^{(j)}$.

The approximated sensitivity (Jacobian matrix) of the component outputs at $\boldsymbol{x}^{(0)}$ can be found in a similar manner as

$$\boldsymbol{J}^{(0)} = s_J(\boldsymbol{F}_t) \tag{4}$$

Figure 2 illustrates the introduced concepts for an exemplary two-dimensional objective space and three-dimensional parameter space. It should be noted that the initial point $\boldsymbol{x}^{(0)}$ obtained from (3) does not coincide with $\boldsymbol{x}^*$ (the design optimum in the sense of (1)) for $\boldsymbol{F} = \boldsymbol{F}_t$. This is because $s_x(F)$ is only an approximation of $O(F)$. Consequently, a design refinement is necessary.

D. BASIC DESIGN REFINEMENT: FAST GRADIENT SEARCH

In this section, a simple design refinement procedure using trust-region (TR)-embedded gradient search is described [27]. This procedure will be used as a reference for the iterative correction scheme of Section II.*E*.

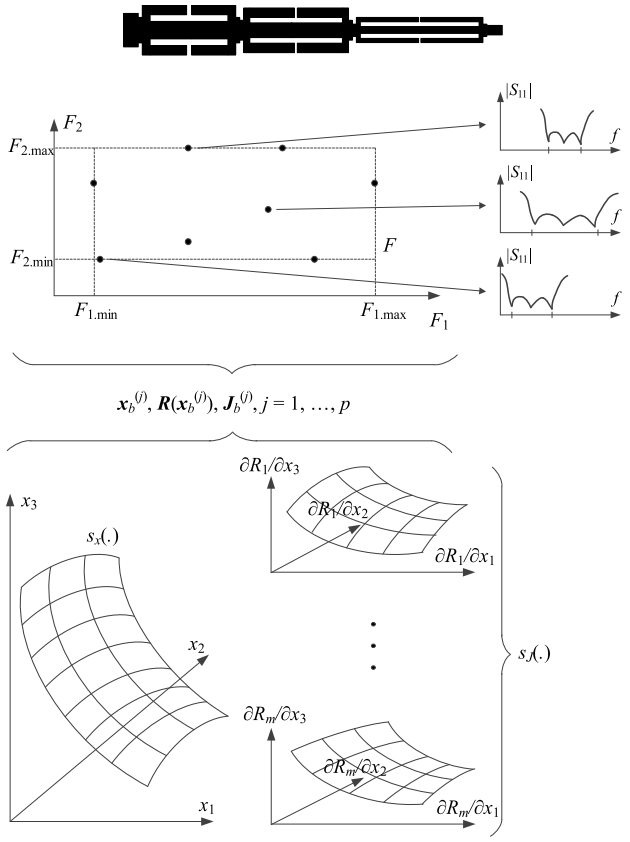

FIGURE 1. Conceptual illustration of the objective space (here, with the operating conditions being the lower and upper ends of the operating frequency band) for a compact three-section impedance matching transformer shown at the top. The frequency characteristics exemplify the transformer reflection optimized for various operating bandwidths, according to the objective vectors allocated within the objective space $\boldsymbol{F}$. The reference designs, corresponding transformer outputs, and their sensitivities are subsequently used to construct the surrogates s_x and s_J, shown as the response surfaces at the bottom part of the picture.

The TR algorithm employs an auxiliary linear model

$$\boldsymbol{L}^{(i)}(\boldsymbol{x}) = \boldsymbol{R}(\boldsymbol{x}^{(i)}) + \boldsymbol{J}_{\boldsymbol{R}}(\boldsymbol{x}^{(i)}) \cdot (\boldsymbol{x} - \boldsymbol{x}^{(i)}) \tag{5}$$

to generate a series $\boldsymbol{x}^{(i)}$, $i = 0, 1, \ldots$, of approximations to the optimum point $\boldsymbol{x}^*$ as

$$\boldsymbol{x}^{(i+1)} = \arg \min_{\boldsymbol{x};\ -\boldsymbol{d}^{(i)} \le \boldsymbol{x} - \boldsymbol{x}^{(i)} \le \boldsymbol{d}^{(i)}} U(\boldsymbol{L}^{(i)}(\boldsymbol{x}), \boldsymbol{F}_t) \tag{6}$$

The construction of model (5) requires the Jacobian matrix $\boldsymbol{J}_{\boldsymbol{R}}$, which is normally estimated through finite differentiation (FD), unless other means, e.g., adjoints sensitivities [15] are available. In this work, the two mechanisms are employed to reduce the computational cost of the process:

- The sensitivity matrix is initialized using the kriging surrogate (cf. (3)) instead of being estimated by FD;
- For $i > 0$, $\boldsymbol{J}_{\boldsymbol{R}}(\boldsymbol{x}^{(i)})$ is updated from $\boldsymbol{J}_{\boldsymbol{R}}(\boldsymbol{x}^{(i-1)})$ using a rank-one Broyden formula [28];

Owing to these, the cost of individual iterations of (6) can be as low as one EM analysis, whereas the entire refinement process can be accomplished using a small number of EM

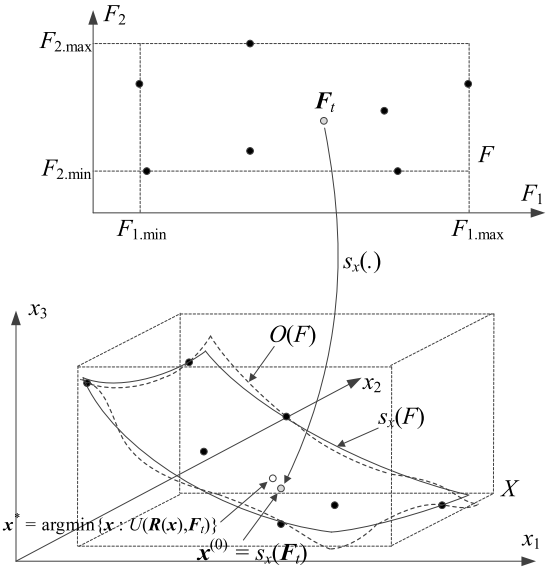

FIGURE 2. Basic concepts of the expedited design optimization procedure. Top: the objective space F and the exemplary target objective vector F_t. Bottom: $s_x(F)$ (solid lines), the set of optimum designs $O(F)$ (dashed lines), and the exemplary initial design $s_x(F_t)$ (gray-shaded circle) corresponding to the target objective vector F_t. Designs $x_b^{(j)}$ and $s_x(x_b^{(j)})$ are marked using black circles. As $s_x(F)$ is an approximation of $x^* = \text{argmin}\{x: U(R(x), F_t)\}$, x^* (white circle) does not coincide with $s_x(F_t)$.

simulations. On the other hand, reliability of (6) depends on the accuracy of $\boldsymbol{J}^{(0)}$ and the distance between $\boldsymbol{x}^{(0)}$ and $\boldsymbol{x}^*$.

E. ITERATIVE DESIGN REFINEMENT

This section formulates an alternative design refinement process involving multiple evaluations of the kriging surrogate model s_x.

Let $\boldsymbol{F}_{tmp.0}$ be the objective vector found by extracting the merit function values from the EM-simulated response of the microwave component of interest at $\boldsymbol{x}^{(0)}$ (cf. (3)). The design inaccuracy, i.e., the difference between the performance figure or operating condition values at $\boldsymbol{x}^{(0)}$ and the target ones can be quantified as $\Delta\boldsymbol{F}^{(0)} = \boldsymbol{F}_{tmp.0} - \boldsymbol{F}_t$.

Using $\Delta\boldsymbol{F}^{(0)}$, the corrected design can be obtained from the surrogate model s_x as

$$\boldsymbol{x}^{(1)} = s_x(\boldsymbol{F}_t - \Delta\boldsymbol{F}^{(0)}) \tag{7}$$

Unfortunately, the optimum design $\boldsymbol{x}^*$ is generally a nonlinear function of the target vector $\boldsymbol{F}_t$, therefore, the correction (7) needs to be repeated. The iterative procedure employs the accumulated errors $\Delta\boldsymbol{F}^{(k)} = \boldsymbol{F}_{tmp.k} - \boldsymbol{F}_t$, where $\boldsymbol{F}_{tmp.k}$ is the vector of objectives extracted from the EM-simulated response of the component under design at the current point $\boldsymbol{x}^{(k)}$. We have

$$\boldsymbol{x}^{(i+1)} = s_x\left(\boldsymbol{F}_t - \sum\nolimits_{k=0}^{i} \Delta\boldsymbol{F}^{(k)}\right) \tag{8}$$

Assuming that the initial design $\boldsymbol{x}^{(0)}$ is of sufficient quality, the process (8) converges quickly. In practice, only a few (two to four) iterations are required. The gradient-based refinement (6) may be subsequently applied as the final stage of the optimization procedure. This is to correct the figures of interest that are not directly controlled by (8). For example, if the figures F_k correspond to the lower/upper ends of the operating bandwidth, the correction (8) would primarily affect the frequency allocation of the bandwidth but not the level of the response (e.g., return loss values). In other words, further design improvement w.r.t. the merit function U requires explicit minimization of $U(\boldsymbol{R}(\boldsymbol{x}), \boldsymbol{F}_t)$ using, e.g., (6).

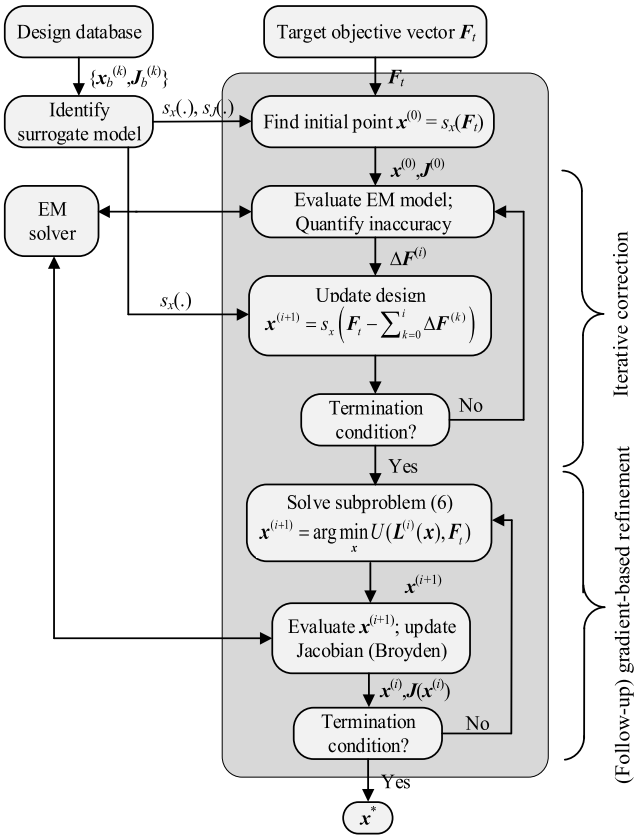

FIGURE 3. Flow diagram of the proposed design closure procedure with iterative refinement scheme.

Notwithstanding, the iterative correction (8) enables relatively large design relocations, which is particularly suitable when correcting the frequency shifts (with respect to, e.g., the target operating bandwidths) of the system outputs at the initial design. This is not straightforward for the gradient-based refinement (6) because the latter only employs roughly estimated sensitivity data. As mentioned before, the important advantage of (8) is its low computational cost of only one EM simulation per iteration.

Figure 3 shows the flow diagram of the entire design closure procedure including the iterative refinement scheme and the follow-up gradient-based optimization.

III. RESULTS

This section provides comprehensive numerical validation of the proposed design closure procedure. It has been applied

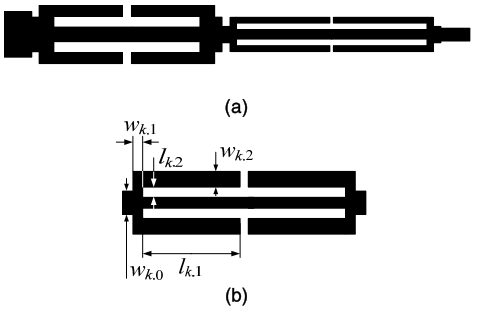

FIGURE 4. CMRC-based compact two-section impedance matching transformer: (a) topology of a two-section structure, (b) compact cell (CMRC).

to the parameter tuning of two impedance matching transformers optimized over wide ranges of operating conditions. Benchmarking against the gradient-based refinement procedure is also included.

A. CASE STUDY I: TWO-SECTION CMRC-BASED IMPEDANCE MATCHING TRANSFORMER

The first verification example is the 50-to-100 ohm impedance matching transformer shown in Fig. 4(a). The circuit is composed of two compact microstrip resonant cells (CMRCs) shown in Fig. 4(b). The circuit is implemented on RF-35 substrate ($\varepsilon_r = 3.5$, $h = 0.762$ mm). The design parameters are $\boldsymbol{x} = [l_{1.1}\ l_{1.2} w_{1.1} w_{1.2}\ w_{1.0} l_{2.1}\ l_{2.2} w_{2.1} w_{2.2}\ w_{2.0}]^T$. The computational model is implemented in CST Microwave Studio and evaluated its time-domain solver (∼270,000 mesh cells, simulation time 140 seconds).

The objective space for the circuit of Fig. 4(a) is defined by the lower end f_1 of the operating frequency range and its upper end Kf_1, with 1.5 GHz $\leq f_1 \leq$ 3.5 GHz, and $1.5 \leq K \leq 2.5$. The design goal is to minimize the in-band reflection of the transformer. The kriging models s_x and s_J are constructed using nine reference designs corresponding to $\{f_1, K\} = \{1.5, 1.5\}, \{1.5, 2.0\}, \{1.5, 2.5\}, \{2.5, 1.5\}, \{2.5, 2.0\}, \{2.5, 2.5\}, \{3.5, 1.5\}, \{3.5, 2.0\}$, and $\{3.5, 2.5\}$. The major challenges of the design problem come from a small number of the reference points as well as a relatively large number of geometry parameters.

The design closure procedure of Section II has been validated by optimizing the transformer for six target objective vectors as indicated in Table 1. The transformer characteristics at the initial designs obtained through (3), as well as those obtained through the iterative correction (8), and the follow-up gradient search (6) have been shown in Fig. 5.

For the sake of comparison, Table 1 also contains the designs found using a gradient-based refinement (6), which turns out to be of inferior quality as compared to the iterative correction procedure. The average improvement in terms of the maximum in-band reflection is almost three decibels.

Furthermore, the computational cost of (8) is low, less than three EM transformer simulations on the average. At the same time, the average cost of the follow-up gradient refinement is

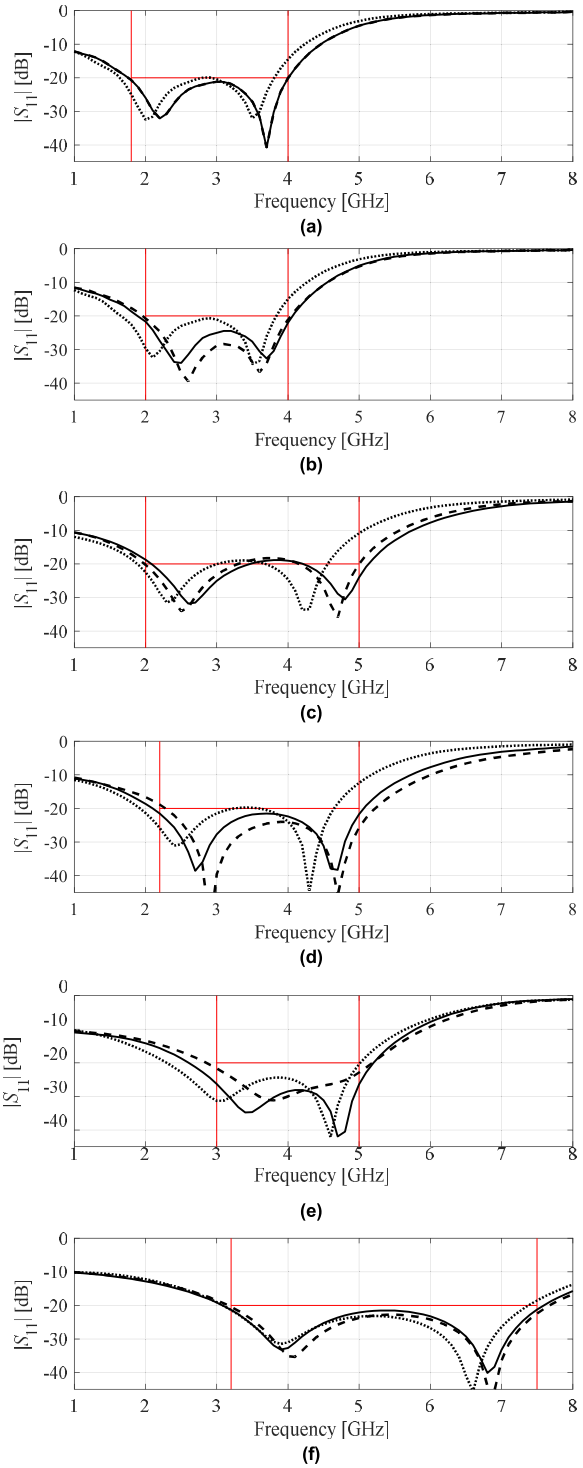

FIGURE 5. Responses of the two-section impedance matching transformer of Fig. 4(a) at the initial design (· · ··), the designs optimized using the iterative correction scheme (- - -), and the final design obtained using the gradient search of Section II.*C* (as a follow up) (—). Shown are designs corresponding to the target vectors of Table 1: (a) $f_1 = 1.8$ GHz, $Kf_1 = 4.0$ GHz, (b) $f_1 = 2.0$ GHz, $Kf_1 = 4.0$ GHz, (c) $f_1 = 2.0$ GHz, $Kf_1 = 5.0$ GHz, (d) $f_1 = 2.2$ GHz, $Kf_1 = 5.0$ GHz, (e) $f_1 = 3.0$ GHz, $Kf_1 = 5.0$ GHz, (f) $f_1 = 3.2$ GHz, $Kf_1 = 7.5$ GHz.

five EM analyses. Consequently, the overall design closure cost corresponds to only around eight EM analyses, which is less than the number of the transformer parameters.

TABLE 1. Optimization results for impedance transformer of Fig. 4.

Test case		1	2	3	4	5	6
Target operating band	f_1 [GHz]	1.8	2.0	2.0	2.2	3.0	3.2
	Kf_1 [GHz]	4.0	4.0	5.0	5.0	5.0	7.5
max$\|S_{11}\|$ [dB] (gradient-based refinement (6))[$]		–15.0	–21.2	–19.0	–13.8	–26.3	–19.2
max$\|S_{11}\|$ [dB] (iterative correction (8))[#]		–20.2	–21.7	–19.0	–21.5	–26.2	–21.3
Geometry parameters [mm]	$l_{1.1}$	3.74	3.69	2.91	2.89	2.53	2.01
	$l_{1.2}$	0.28	0.17	0.14	0.54	0.21	0.15
	$w_{1.1}$	0.77	0.60	0.76	0.80	0.55	0.95
	$w_{1.2}$	0.29	0.61	0.33	0.10	0.80	0.13
	$w_{1.0}$	0.22	0.23	0.48	0.20	0.54	0.35
	$l_{2.1}$	4.26	4.46	3.75	4.51	3.99	2.78
	$l_{2.2}$	0.48	0.42	0.34	0.10	0.16	0.13
	$w_{2.1}$	0.38	0.42	0.49	0.52	0.48	0.55
	$w_{2.2}$	0.23	0.15	0.18	0.16	0.20	0.11
	$w_{2.0}$	0.65	0.80	0.27	1.12	0.55	0.29

[$] maximum in-band reflection obtained when using gradient-based refinement (6).
[#] maximum in-band reflection obtained when using iterative correction (8) followed-up by gradient search (6).

FIGURE 6. Geometry of the three-section impedance matching transformer.

B. CASE STUDY II: THREE-SECTION CMRC-BASED IMPEDANCE MATCHING TRANSFORMER

The second verification example is a compact three-section 50-to-100 Ohm impedance matching transformer shown in Fig. 6(a) and implemented on the RF-35 substrate. Similarly as in the case of the circuit of Fig. 4(a), a reduction of the physical length of the structure is obtained by replacing conventional transmission lines with the compact microstrip resonant cells (CMRCs) shown in Fig. 4(b).

The circuit is implemented on RF-35 substrate ($\varepsilon_r = 3.5$, $h = 0.762$ mm) and described by fifteen parameters $\boldsymbol{x} = [l_{1.1}$ $l_{1.2}w_{1.1}w_{1.2}$ $w_{1.0}l_{2.1}$ $l_{2.2}w_{2.1}w_{2.2}$ $w_{2.0}l_{3.1}$ $l_{3.2}w_{3.1}w_{3.2}$ $w_{3.0}]^T$.

The objective space is determined by the intended operating bands $[f_1\ f_2]$ within which the reflection $|S_{11}|$ is to be minimized. The ranges of interest for f_1 and f_2 are as follows: 1.5 GHz $\leq f_1 \leq$ 3.5 GHz, and 4.5 GHz $\leq f_2 \leq$ 6.5 GHz. The kriging surrogates are constructed using five reference designs $\boldsymbol{x}_b^{(j)}$, corresponding to $\{f_1, f_2\} = \{1.5, 4.5\}, \{1.5, 6.5\}, \{2.5, 5.5\}, \{3.5, 4.5\}$, and $\{3.5, 6.5\}$ (frequencies in GHz). Note that the number of reference designs is very small. This, in conjunction with high dimensionality of the parameter space, contribute to the major challenges of the design task.

The presented design optimization procedure has been applied to optimize the transformer circuit for six target objective vectors as listed in Table 2. Figure 7 shows the transformer characteristics at the initial designs obtained using (3), we well as upon iterative correction (8) and the follow-up gradient search (6).

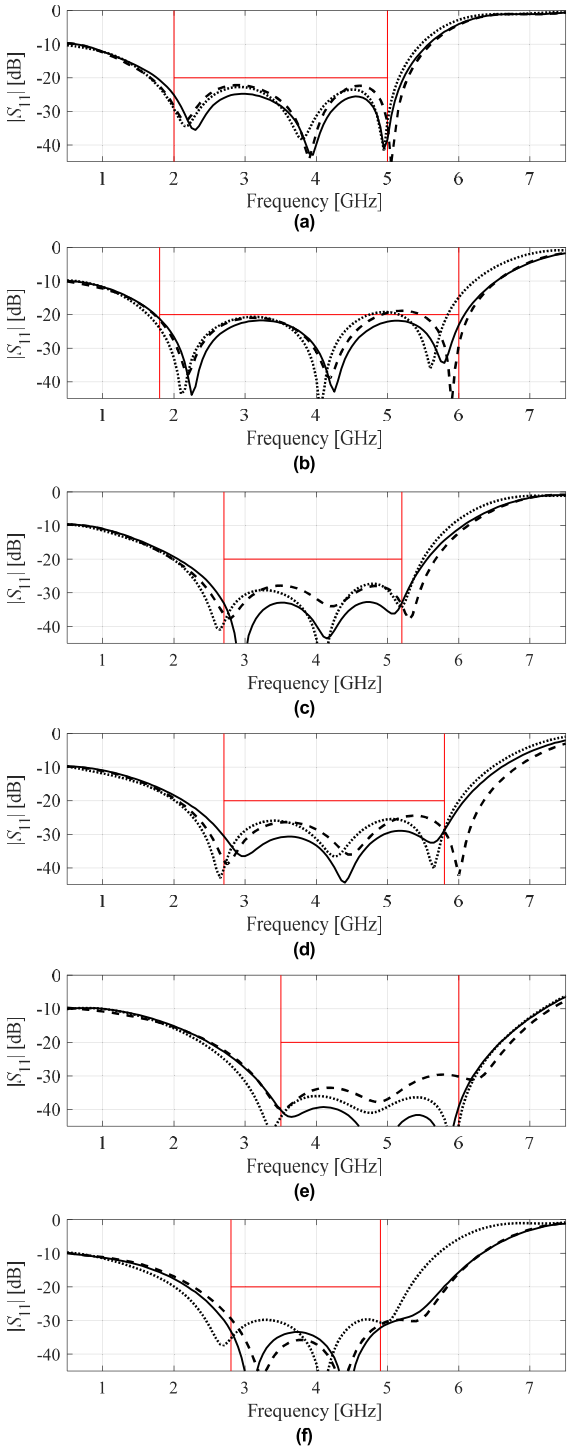

FIGURE 7. Impedance matching transformer responses at the initial design (· · ·), the designs optimized using the iterative correction scheme (- - -), and the final design obtained using the gradient search of Section II.C (as a follow up) (—). Shown are designs corresponding to the target vectors of Table 2: (a) $f_1 = 2.0$ GHz, $f_2 = 5.0$ GHz, (b) $f_1 = 1.8$ GHz, $f_2 = 6.0$ GHz, (c) $f_1 = 2.7$ GHz, $f_2 = 5.2$ GHz, (d) $f_1 = 2.7$ GHz, $f_2 = 5.8$ GHz, (e) $f_1 = 3.5$ GHz, $f_2 = 6.0$ GHz, (f) $f_1 = 2.8$ GHz, $f_2 = 4.9$ GHz.

The data in Table 2 indicates that the iterative correction scheme ensures a better design quality than the gradient search alone. The average improvement in terms of the

TABLE 2. Optimization results for impedance transformer of Fig. 6.

Test case		1	2	3	4	5	6
Target operating band	f_1 [GHz]	2.0	1.8	2.7	2.7	3.5	2.8
	f_2 [GHz]	5.0	6.0	5.2	5.8	6.0	4.9
max$\|S_{11}\|$ [dB] (gradient-based refinement (6))[$]		–23.3	–19.3	–30.1	–28.9	–36.0	–31.4
max$\|S_{11}\|$ [dB] (iterative correction (8))[#]		–24.8	–21.3	–32.7	–28.9	–39.1	–32.3
Geometry parameters [mm]	$l_{1.1}$	2.95	2.91	2.76	2.42	2.12	2.33
	$l_{1.2}$	0.30	0.18	0.21	0.27	0.34	0.34
	$w_{1.1}$	0.75	0.80	0.80	0.80	0.80	0.79
	$w_{1.2}$	0.50	0.44	0.55	0.53	0.55	0.49
	$w_{1.0}$	1.14	0.53	0.72	0.61	0.87	1.00
	$l_{2.1}$	3.60	3.48	3.62	3.31	3.12	3.19
	$l_{2.2}$	0.33	0.18	0.17	0.17	0.20	0.21
	$w_{2.1}$	0.55	0.64	0.57	0.62	0.66	0.55
	$w_{2.2}$	0.23	0.15	0.25	0.24	0.18	0.30
	$w_{2.0}$	0.73	0.31	0.81	0.51	0.75	0.98
	$l_{3.1}$	4.03	3.67	3.77	3.53	3.21	3.60
	$l_{3.2}$	0.19	0.16	0.15	0.16	0.15	0.16
	$w_{3.1}$	0.36	0.42	0.34	0.36	0.35	0.32
	$w_{3.2}$	0.20	0.15	0.15	0.15	0.15	0.18
	$w_{3.0}$	0.70	0.81	1.00	0.77	0.30	0.56

[$] maximum in-band reflection obtained when using gradient-based refinement (6).
[#] maximum in-band reflection obtained when using iterative correction (8) followed-up by gradient search (6).

maximum in-band reflection is almost 2 dB. At the same time, the average cost of (8) is four EM simulations of the transformer circuit, whereas the average cost of the follow-up gradient refinement is 4.5 EM analyses. Thus, the total cost of the optimization process is less than nine transformer simulations on the average.

IV. CONCLUSION

The paper proposed a novel surrogate-assisted technique for expedited design closure of miniaturized microwave components. Our methodology exploits two kriging interpolation metamodels constructed from a set of pre-optimized reference designs. For a given target vector of objectives, the models allow us to render a good initial point and to jump-start the gradient-based design refinement procedure. Furthermore, a dedicated iterative correction scheme has been developed to permit rapid design improvements, especially in terms of accommodating the frequency shifts that occur due to surrogate model inaccuracies.

Comprehensive numerical verification conducted for two miniaturized impedance matching transformer circuits (a two- and a three-section one) demonstrates the efficacy of the proposed approach in terms of its capability of yielding a satisfactory design for any target vector of figures of interest within the region of validity of the method. This is achieved at a low computational cost corresponding to a few EM analyses of the circuit at hand.

Our technique might be useful to reduce the CPU cost of parameter tuning procedures whenever a set of previously obtained designs is available or the initial effort related to pre-optimization of such designs may be justified by the planned reuse of the framework.

ACKNOWLEDGMENT

The authors thank Dassault Systemes, France, for making CST Microwave Studio available.

REFERENCES

[1] F. Feng, C. Zhang, W. Na, J. Zhang, W. Zhang, and Q.-J. Zhang, "Adaptive feature zero assisted surrogate-based EM optimization for microwave filter design," *IEEE Microw. Wireless Compon. Lett.*, vol. 29, no. 1, pp. 2–4, Jan. 2019.
[2] Z. Medina, A. Reyna, M. A. Panduro, and O. Elizarraras, "Dual-band performance evaluation of time-modulated circular geometry array with microstrip-fed slot antennas," *IEEE Access*, vol. 7, pp. 28625–28634, 2019.
[3] Z. Chen, Y. Xu, B. Zhang, T. Chen, T. Gao, and R. Xu, "A GaN HEMTs nonlinear large-signal statistical model and its application in S-band power amplifier design," *IEEE Microw. Wireless Compon. Lett.*, vol. 26, no. 2, pp. 128–130, Feb. 2016.
[4] J. Zhang, C. Zhang, F. Feng, W. Zhang, J. Ma, and Q.-J. Zhang, "Polynomial chaos-based approach to yield-driven EM optimization," *IEEE Trans. Microw. Theory Techn.*, vol. 66, no. 7, pp. 3186–3199, Jul. 2018.
[5] A. Contreras, M. Ribo, L. Pradell, V. Raynal, I. Moreno, M. Combes, and M. Ten, "Compact fully uniplanar bandstop filter based on slow-wave multimodal CPW resonators," *IEEE Microw. Wireless Compon. Lett.*, vol. 28, no. 9, pp. 780–782, Sep. 2018.
[6] H. Zhu and A. M. Abbosh, "A compact tunable directional coupler with continuously tuned differential phase," *IEEE Microw. Wireless Compon. Lett.*, vol. 28, no. 1, pp. 19–21, Jan. 2018.
[7] C. W. Byeon and C. S. Park, "Low-loss compact millimeter-wave power divider/combiner for phased array systems," *IEEE Microw. Wireless Compon. Lett.*, vol. 29, no. 5, pp. 312–314, May 2019.
[8] C.-F. Chen, S.-F. Chang, and B.-H. Tseng, "Compact microstrip dual-band quadrature coupler based on coupled-resonator technique," *IEEE Microw. Wireless Compon. Lett.*, vol. 26, no. 7, pp. 487–489, Jul. 2016.
[9] S. Koziel and P. Kurgan, "Inverse modeling for fast design optimization of small-size rat-race couplers incorporating compact cells," *Int. J. RF Microw. Comput.-Aided Eng.*, vol. 28, no. 5, Jun. 2018, Art. no. e21240.
[10] H. Jin, Y. Zhou, Y. M. Huang, S. Ding, and K. Wu, "Miniaturized broadband coupler made of slow-wave half-mode substrate integrated waveguide," *IEEE Microw. Wireless Compon. Lett.*, vol. 27, no. 2, pp. 132–134, Feb. 2017.
[11] Z. Zeng, Y. Yao, and Y. Zhuang, "A wideband common-mode suppression filter with compact-defected ground structure pattern," *IEEE Trans. Electromagn. Compat.*, vol. 57, no. 5, pp. 1277–1280, Oct. 2015.
[12] H.-W. Wu and C.-T. Chiu, "Design of compact multi-layered quad-band bandpass filter," *IEEE Microw. Wireless Compon. Lett.*, vol. 26, no. 11, pp. 879–881, Nov. 2016.
[13] R. Gomez-Garcia, J. Rosario-De Jesus, and D. Psychogiou, "Multi-band bandpass and bandstop RF filtering couplers with dynamically-controlled bands," *IEEE Access*, vol. 6, pp. 32321–32327, 2018.
[14] R. K. Barik, R. Rajender, and S. S. Karthikeyan, "A miniaturized wideband three-section branch-line hybrid with harmonic suppression using coupled line and open-ended stubs," *IEEE Microw. Wireless Compon. Lett.*, vol. 27, no. 12, pp. 1059–1061, Dec. 2017.
[15] H. Malhi and M. H. Bakr, "Geometry evolution of microwave filters exploiting self-adjoint sensitivity analysis," in *Proc. Int. Conf. Numerical Electromagn. Multiphys. Mod. Opt. (NEMO)*, Ottawa, ON, Canada, Aug. 2015, pp. 11–14.
[16] S. Koziel, Q. S. Cheng, J. W. Bandler, and S. Ogurtsov, "Rapid electromagnetic-based microwave design optimisation exploiting shape-preserving response prediction and adjoint sensitivities," *IET Microw., Antennas Propag.*, vol. 8, no. 10, pp. 775–781, Jul. 2014.
[17] A. Pietrenko-Dabrowska and S. Koziel, "Computationally-efficient design optimisation of antennas by accelerated gradient search with sensitivity and design change monitoring," *IET Microw., Antennas Propag.*, vol. 14, no. 2, pp. 165–170, Feb. 2020.

[18] A. Pietrenko-Dabrowska and S. Koziel, "Numerically efficient algorithm for compact microwave device optimization with flexible sensitivity updating scheme," *Int. J. RF Microw. Comput.-Aided Eng.*, vol. 29, no. 7, Jul. 2019, Art. no. e21714.
[19] H. M. Torun and M. Swaminathan, "High-dimensional global optimization method for high-frequency electronic design," *IEEE Trans. Microw. Theory Techn.*, vol. 67, no. 6, pp. 2128–2142, Jun. 2019.
[20] J. E. Rayas-Sanchez, "Power in simplicity with ASM: Tracing the aggressive space mapping algorithm over two decades of development and engineering applications," *IEEE Microw. Mag.*, vol. 17, no. 4, pp. 64–76, Apr. 2016.
[21] S. Koziel and A. Bekasiewicz, "Rapid microwave design optimization in frequency domain using adaptive response scaling," *IEEE Trans. Microw. Theory Techn.*, vol. 64, no. 9, pp. 2749–2757, Sep. 2016.
[22] S. Koziel, "Fast simulation-driven antenna design using response-feature surrogates," *Int. J. RF Microw. Comput.-Aided Eng.*, vol. 25, no. 5, pp. 394–402, Jun. 2015.
[23] S. J. Mahon and D. J. Skellern, "Procedure for inverse modelling of GaAs/AlGaAs HEMT structures from DC I/V characteristic curves," *Electron. Lett.*, vol. 27, no. 1, pp. 81–82, Jan. 1991.
[24] S. Koziel and A. Bekasiewicz, "Expedited geometry scaling of compact microwave passives by means of inverse surrogate modeling," *IEEE Trans. Microw. Theory Techn.*, vol. 63, no. 12, pp. 4019–4026, Dec. 2015.
[25] S. Koziel and A. Bekasiewicz, "Inverse and forward surrogate models for expedited design optimization of unequal-power-split patch couplers," *Metrol. Meas. Syst.*, vol. 26, no. 3, pp. 463–473, 2019.
[26] N. V. Queipo, R. T. Haftka, W. Shyy, T. Goel, R. Vaidynathan, and P. K. Tucker, "Surrogate-based analysis and optimization," *Progr. Aerosp. Sci.*, vol. 41, no. 1, pp. 1–28, Jan. 2005.
[27] A. R. Conn, N. I. M. Gould, and P. L. Toint, *Trust Region Methods* (MPS-SIAM Series on Optimization), Philadelphia, PA, USA: SIAM, 2000.
[28] C. G. Broyden, "A class of methods for solving nonlinear simultaneous equations," *Math. Comput.*, vol. 19, no. 92, pp. 577–593, 1965.

SLAWOMIR KOZIEL (Senior Member, IEEE) received the M.Sc. and Ph.D. degrees in electronic engineering from the Gdańsk University of Technology, Poland, in 1995 and 2000, respectively, the M.Sc. degrees in theoretical physics and mathematics, in 2000 and 2002, respectively, and the Ph.D. degree in mathematics from the University of Gdańsk, Poland, in 2003. He is currently a Professor with the Department of Technology, Reykjavik University, Iceland. His research interests include CAD and modeling of microwave and antenna structures, simulation-driven design, surrogate-based optimization, space mapping, circuit theory, analog signal processing, evolutionary computation, and numerical analysis.

ANNA PIETRENKO-DABROWSKA (Member, IEEE) received the M.Sc. and Ph.D. degrees in electronic engineering from the Gdańsk University of Technology, Poland, in 1998 and 2007, respectively. She is currently an Associate Professor with the Gdańsk University of Technology. Her research interests include simulation-driven design, design optimization, control theory, modeling of microwave and antenna structures, and numerical analysis.